Gold Nanoparticle Photopolymerization of Acrylates

Kelechi C. Anyaogu, Xichen Cai, and Douglas C. Neckers*

Center for Photochemical Sciences, Bowling Green State University, Bowling Green, Ohio 43403

Received June 20, 2008; Revised Manuscript Received September 19, 2008

ABSTRACT: We report the photochemical incorporation of stabilized gold nanoparticles (AuNPs) into a polymer matrix without the use of conventional photoinitiators. AuNPs in the size range of 2−6 nm are modified with 5-mercapto-2,2′-bithiophene. The charge-separated states of the functionalized AuNPs generated upon exposure to UV light are active intermediates that can cause polymerization of an acrylic monomer. Photopolymerization was monitored by near Fourier transform infrared measurements. Scanning electron microscopy reveals uniform distribution of the AuNPs within the matrix and a unique texture of the polymer composite.

Introduction

Metal nanoparticle−polymer composites have attracted intense research interest in recent years.[1−4] The incorporation of nanoparticles into polymers has created a new generation of materials exhibiting unique electrical, optical, or mechanical properties which make them attractive for applications in areas like optics,[5] photoimaging and patterning,[6] sensor design,[7] catalysis,[8] and as antimicrobial coatings.[9−11] Several strategies have been reported for the preparation of nanoparticle−polymer composites. A common approach involves mechanical dispersion of premade nanoparticles into a polymer matrix[12] or in situ preparation of the nanoparticles within the matrix by reduction of metal salts.[13,14] Another technique involves polymerizing the matrix around a metal nanocore by using chemically compatible ligands[15,16] or polymeric structures.[17] Mills et al.[18] reported photogeneration of silver nanoparticles in PVA matrix, the metal ions being reduced by the polymeric benzophenone ketyl radicals. Later reports by Rizza et al. describe photoinduced synthesis of silver−epoxy nanocomposites.[19] A key challenge, however, remains the homogeneous dispersion of the nanoparticles and their stability within the matrix.[20]

In this paper, we report the photochemical incorporation of 5-mercapto-2,2′-bithiophene functionalized gold nanoparticles (BTSAuNPs) of sizes ∼2, 4, and 6 nm into a polymeric matrix. The photopolymerization of an acrylic monomer results from exposure of BTSAuNPs to UV light and, thus, does not require the use of conventional photoinitiators. Bithiophene radical cation [$^{\bullet+}$BTSAuNP(e)] is generated by intramolecular electron transfer during the UV light irradiation.[21] The NPs were characterized by transmission electron micrsocopy (TEM), UV−vis spectroscopy, Fourier transform infrared (FTIR), and energy dispersive X-ray (EDX) analysis. Scanning electron microscopy (SEM) was used to characterize the nanoparticle−polymer composites. The SEM images show a uniform distribution of the NPs within the matrix. And, interestingly, the NP−polymer composite surface and cross section display a unique textural pattern different from that observed using a conventional photoinitiator.

Experimental Section

Materials. Gold(III) chloride trihydrate ($HAuCl_4 \cdot 3H_2O$), 1-dodecanethiol (98%), and tetraoctylammonium bromide $N(C_8H_{17})_4Br$ (98%) were purchased from Aldrich. Monofunctional (2-phenoxyethyl acrylate − SR 339), difunctional (dipropylene glycol diacrylate − SR 508), and trifunctional (trimethylolpropane triacrylate − SR 351) acrylates were obtained from Sartomer. Bis(2,4,6-trimethylbenzoyl)phenylphosphine oxide (Irgacure 819) was obtained from Ciba Specialty Chemicals, Inc. 5-Mercapto-2,2′-bithiophene (BTSH) was synthesized based on literature reports.[22,23] All reagents and solvents were used without further purification.

Nanoparticle Preparation. The functionalized AuNPs were prepared using a modified Brust method.[24,25]Typically, an aqueous solution of $HAuCl_4 \cdot 3H_2O$ (0.1 mmol) was added to a round-bottom flask. A toluene solution of tetraoctylammonium bromide, $N(C_8H_{17})_4Br$ (0.22 mmol), was added with rapid stirring. A two-layer separation phase was formed. The ligand (BTSH: 0.2, 0.033, or 0.017 mmol) was added to the solution based on the target diameters of the nanoparticles. Then $NaBH_4$ [aqueous solution (1.1 mmol)] was added dropwise to the mixture with constant stirring. The color of the organic phase changed quickly to reddish-orange and then to blackish-brown. The mixture was stirred for about 12 h. After reaction, the organic phase was separated from the aqueous phase and concentrated using a rotavapor to ∼5 mL. Then 350 mL of 95% ethanol was added, and the mixture was kept in the refrigerator overnight to effect precipitation. The dark black-brown precipitate was filtered and washed with 95% ethanol. The resulting BTSAuNP residue was vacuum-dried and ultrasonically redissolved in toluene.

Characterization. TEM was performed using a ZEISS EM10 transmission electron microscope operating at 80 kV. NP solutions were dropcast (3−4 drops) onto 300-mesh copper grids coated with Formvar and carbon and then air-dried. Size and morphological analysis of the NPs was done manually on no fewer than 200 particles. A diffraction grating replica was used to calibrate the TEM images. UV−vis spectra were recorded on a Shimadzu MultiSpec-1501 spectrometer. FTIR spectra were recorded on a Shimadzu 8400 Series spectrometer. SEM images were recorded on an FEI Quanta Inspect F electron microscope at 5 kV.

Photopolymerization of Acrylic Monomers Using BTSAuNPs. Toluene solutions of the NPs (10 mL) were mixed with the acrylic monomer (10 mmol). This was followed by evaporation of solvent in a rotavapor (∼1 wt % of NPs). Photopolymerization resulted when the liquid formulation (0.1 mL) in an IR cell equipped with rectangular CaF_2 windows (38.5 × 19.5 × 4 mm) and a 1 mm Teflon spacer was irradiated with a 350 nm UV light (RMR-600 Rayonet light source; 85 mm irradiation distance). Near-IR spectroscopy measurements were used to monitor the monomer double-bond conversion (%DB). The spectra were recorded in the range from 5000 to 6500 cm^{-1} with 30 scans and 2 cm^{-1} resolution. The %DB at the respective irradiated times were evaluated by measuring the area ratios between the peaks in the olefinic (6100−6300 cm^{-1}) and aliphatic (5500−6100 cm^{-1}) regions of the first overtone of the CH stretch and compared to those from the unexposed sample.[26,27] Slightly tacky polymer films (∼8 mm thick) were obtained from monomers after 60% double-bond conversion. All manipulations, including NP preparation, were done at room temperature and carefully carried out in the dark prior to irradiation with the UV light.

* To whom correspondence should be addressed: E-mail neckers@photo.bgsu.edu; Tel 419-372-2034; Fax 419-372-0366.

10.1021/ma801391p CCC: $40.75
Published on Web 11/13/2008

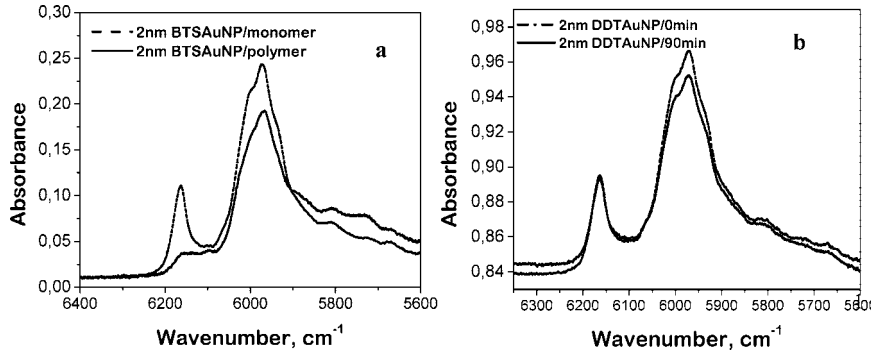

Figure 1. Near-IR spectra of (a) 2 nm BTSAuNPs/2-phenoxyethyl acrylate formulation before (dashed line) and after (solid line) exposure to 350 nm light showing ~56% DB conversion and (b) 2 nm DDTAuNPs/2-phenoxyethyl acrylate formulation before (dashed line) and after (solid line) exposure to 350 nm light for 90 min.

Scheme 1. Schematic Mechanism for the Photopolymerization of Acrylic Monomer Using Bithiophene-Functionalized Gold Nanoparticles (BTSAuNPs); Ar(R) = Aromatic/Aliphatic

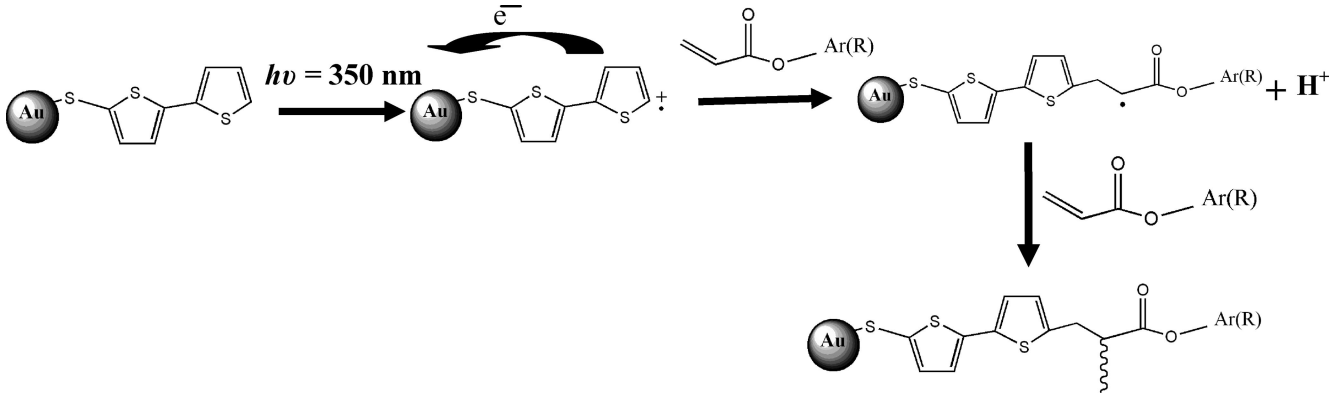

Results and Discussion

Figure 1a shows the near-IR spectra for the unexposed BTSAuNPs/2-phenoxyethyl acrylate mixture and the polymerized matrix obtained after 90 min of exposure to 350 nm light. A significant reduction in the intensity of the olefinic CH region after the UV irradiation can be observed. Control experiments verified this polymerization is not due to the acrylic monomer because irradiating of only the monomer under similar conditions evidenced no double-bond conversion (Figure S4, Supporting Information). 1-Dodecanethiol functionalized gold nanoparticles (DDTAuNPs) do not initiate the polymerization of the acrylic monomer either (Figure 1b), indicating that the active initiating species comes from the charge-separated state [$^{\bullet+}$BTSAuNP(e)] generated upon exposure of the particles to the UV light.[21] Scheme 1 shows the proposed mechanism for the photopolymerization of an acrylic monomer using BTSAuNP. Since the radical cation is localized on the thiophene ring and has a lifetime of ~130 ns in toluene solution,[21] acrylates are not as electron rich as the aromatic thiophene, and the deprotonation of [$^{\bullet+}$BTSAuNP(e)] would produce the unstable aryl radical [$^{\bullet}$BTSAuNP]; the ensuing polymerization likely occurs at the α position of the thiophene[28] by reaction first of the acrylate and then deprotonation. The reactivity patterns of different radical cations have been extensively studied,[29] and in many cases, they are precursors of organic radicals.[30] In this case, however, the encumbering nanoparticle greatly reduces the rate of diffusion, and this also slows the rate of reaction with the acrylate. Using elemental analysis calculations,[31] 2 nm size $^{\bullet+}$BTSAuNP(e) is ca. 300 times heavier than a bithiophene radical cation. Reports[32] show, however, that the rate constant for charge recombination of bithiophene radical cations is in the order ~10^{10}.

Bimolecular rate constants of reactions of substituted phenyl radicals with an acrylate have been reported (~10^8 M^{-1} s^{-1}).[33] We estimate the rate constant of reaction of $^{\bullet+}$BTSAuNP(e) with 2-phenoxyethyl acrylate to be 6.2×10^3 $M^{-1}s^{-1}$. Such a slow reaction rate could be due to quick, competing charge recombination or size of $^{\bullet+}$BTSAuNP(e) which limits diffusion. It is therefore suggested that the acrylate assists in the deprotonation at the α-position of the thiophene ring. The results of photopolymerization with other acrylic monomers are presented in Figure 2a. Dipropylene glycol diacrylate (DPGDA) displayed a higher conversion rate than the other monomers. 68% for DPGDA and 56% double bond conversion for 2-phenoxyethyl acrylate was achieved after 90 min of irradiation with the 350 nm UV light. Because DPGDA is slightly more viscous than 2-phenoxyethyl acrylate,[34] viscosity increases during polymerization, thereby reducing the diffusion of the initiating species; 2-phenoxyethyl acrylate displayed a higher %DB at the end of the irradiation period. Trimethylolpropane triacrylate (TMPTA) showed the lowest degree of conversion, 30%. This slow reactivity may be related to the high viscosity of TMPTA as well as its cross-linking properties.[34]

Figure 2b shows the cure profiles achieved with nanoparticles of different sizes using 2-phenoxyethyl acrylate. This acrylic monomer is known for its low volatility, good adhesion properties, and wide applicability.[34] The fastest double-bond conversion profile was observed with 2 nm BTSAuNPs, and these particles also showed the highest %DB (~60%) after 120 min of irradiation. The 4 nm particles displayed better polymerization rates than the 6 nm size particles. These differences could be related to the intramolecular electron transfer rate in BTSAuNP which decreases with increasing nanoparticle size[21] or the actual size[35] of the active intermediate.

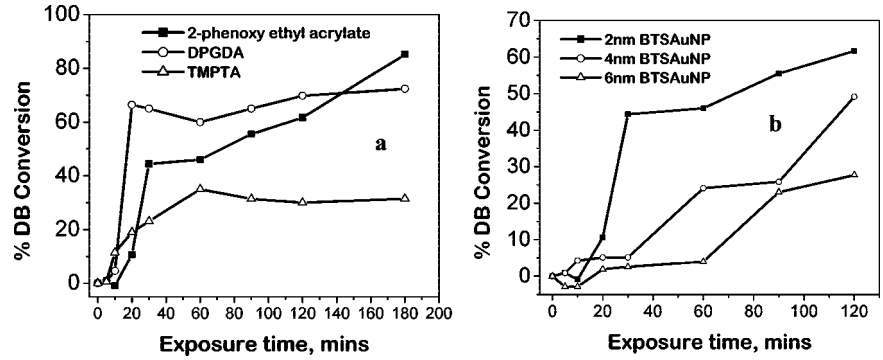

Figure 2. Double-bond conversion curves for (a) 2-phenoxyethyl acrylate (squares), dipropylene glycol diacrylate (circles), and trimethylolpropane triacrylate (triangles) cured using 2 nm BTSAuNPs and (b) 2-phenoxyethyl acrylate cured using 2 nm (squares), 4 nm (circles), and 6 nm (triangles) BTSAuNPs after 350 nm UV light irradiation. The formulations were prepared under the same conditions, and each point on the cure profiles corresponds to an average of at least three measurements.

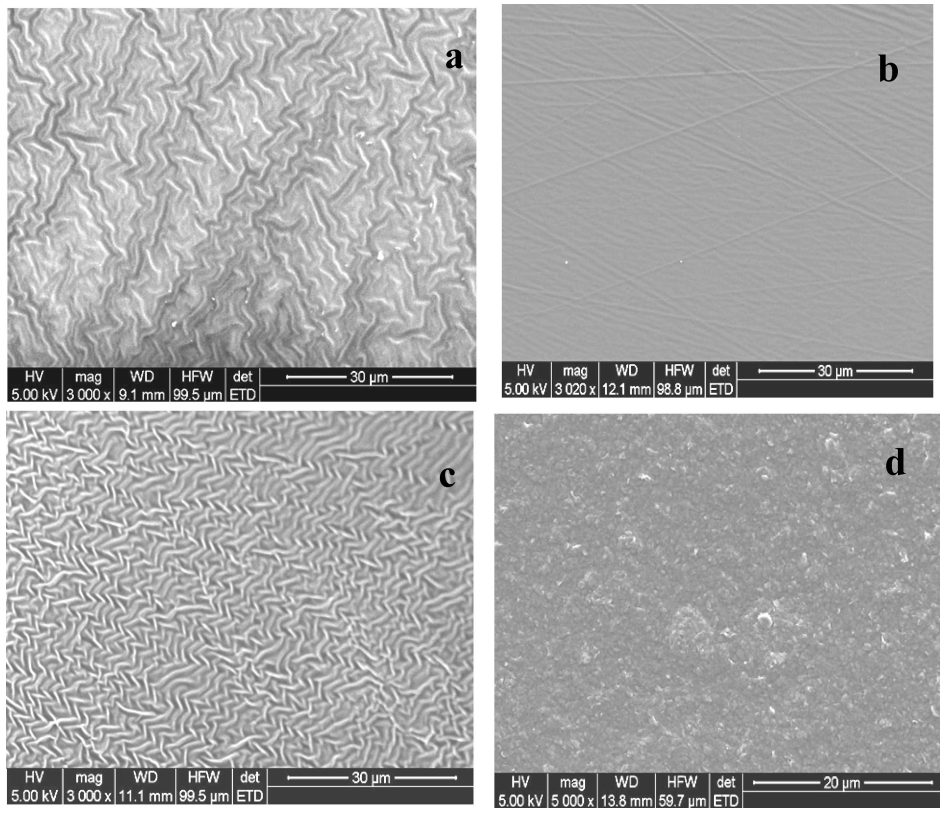

Figure 3. SEM images of surfaces (top) and cross sections (bottom) of polymers (2-phenoxyethyl acrylate) cured with 4 nm BTSAuNPs (a and c) or conventional photoinitiator (b and d).

The surface and cross section of the NP−polymer films were analyzed using SEM. To examine the cross-sectional area, polymer samples were freeze-dried, fractured, and held in place on a hollow aluminum sample holder with graphite glue. For polymer surface analysis, tack-free samples were simply fixed on a flat sample holder with a double-sticker tape. Samples were then coated with carbon (Denton BTT IV vacuum evaporator) before viewing under a microscope (Figure 3). There is a clear difference in morphology between the BTSAuNP/polymer composite and that polymer obtained using the conventional photoinitiator Irgacure 819 (0.2 wt %). A wavy surface and cross-sectional texture can be observed for the BTSAuNP/polymer (Figure 3a,c), whereas the conventional polymer matrix has a rather smooth surface but a rougher cross section (Figure 3b,d). Further analysis of the NP/polymer composite revealed a uniform distribution of the gold nanoparticles within the polymer matrix as shown by the backscattered electron images (BEI, Figure 4) by SEM. The bright spots on the image were confirmed by EDX (INCA, Oxford, Inc.) and found to be from the AuNPs (Figure S6, Supporting Information).

Morphological differences of the polymers could be related to the chemical nature of the initiating intermediates. Since BTSAuNP acts as a photoinitiator during the UV light irradiation, it is expected to be covalently linked to the polymeric backbone. This has obvious advantages[36] over the common mechanical dispersion of nanoparticles in polymer matrices where particle aggregation is virtually unavoidable subsequently strongly affecting the properties of the nanocomposites.[37] When BTSAuNP is chemically linked to the polymer matrix, there is no loss in conformational entropy[3] that may be caused by the polymer chain stretch around the nanoparticle; therefore, a good distribution of the gold nanoparticles within the matrix is achieved (Figure 4a). The wavy surface and cross-sectional texture observed for the BTSAuNP/polymer composite may also be due to the covalent attachment of BTSAuNP to the polymer matrix. From a control experiment, no unique textural patterns

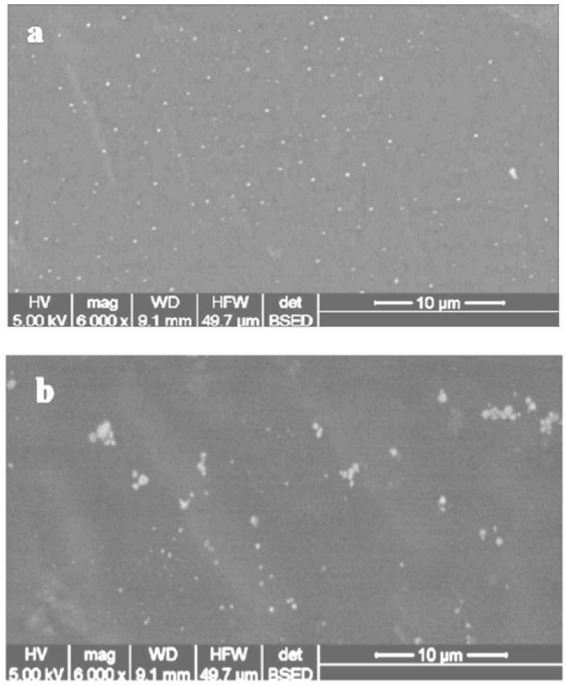

Figure 4. Backscattered electron images of NP/polymer composites polymerized by (a) 4 nm BTSAuNPs and (b) Irgacure 819 with DDTAuNPs embedded in the matrix.

were observed when DDTAuNPs were embedded in the acrylic monomer and polymerized using conventional photoinitiator (Figure 4b and Figure S7 in the Supporting Information). On the other hand, because BTSAuNPs are presynthesized, particle size can be controlled. This also has advantage over the in situ preparation of nanoparticles within a matrix, in which the particles can have a relatively large size distribution.[14a,19]

In summary, we demonstrated the photochemical incorporation of gold nanoparticles into a polymer matrix. AuNPs are functionalized with 5-mercapto-2,2′-bithiophene. The $^{\bullet+}$BTSAuNP(e) is active intermediate that can cause polymerization of an acrylic monomer. Good spatial distribution of the nanoparticles within the polymer matrix can be achieved. The efficiency of the photopolymerization maybe related to the rate of intramolecular electron transfer, size, or concentration of the active intermediates. Additional studies on particle size and concentration effects on the photopolymerization are underway.

Acknowledgment. The authors thank the Office of Naval Research for financial support (Grant N00014-04-1-0406). This is Contribution No. 696 from the Center for Photochemical Sciences.

Supporting Information Available: UV−vis spectra, TEM images, EDX spectra, near-IR spectra, additional SEM images, and chemical structures of tested monomers and photoinitiator. This material is available free of charge via the Internet at http://pubs.acs.org.

References and Notes

(1) Thomas, V.; Namdeo, M.; Murali, M. Y.; Bajpai, S. K.; Bajpai, M. *J. Macromol. Sci., Pure Appl. Chem. A* **2008**, *45*, 107–119.
(2) Carotenuto, G.; Nicolais, L. *Metal-Polymer Nanocomposites*; Wiley: New York, 2005; Chapter 5.
(3) (a) Thompson, R. B.; Ginzburg, V. V.; Matsen, M. W.; Balazs, A. C. *Science* **2001**, *292*, 2469–2472. (b) Russel, T. P.; Emrick, T.; Balazs, A. C. *Science* **2006**, *314*, 1107–1110.
(4) Boal, A. K.; Ilhan, F.; De Rouchey, J. E.; Thurn-Albrecht, T.; Russel, T. P.; Rotello, V. M. *Nature (London)* **2000**, *404*, 746–748.
(5) José-Yacamán, M.; Pérez, R.; Santiago, P.; Benaissa, M.; Gonsalves, K.; Carlson, G. *Appl. Phys. Lett.* **1996**, *69*, 913–915.
(6) Stellacci, F.; Bauer, C. A.; Meyer-Friedrichsen, T.; Wenseleers, W.; Alain, V.; Kuebler, S. M.; Pond, S. J. K.; Zhang, Y.; Marder, S. R.; Perry, J. W. *Adv. Mater.* **2002**, *14*, 194–198.
(7) Zamborini, F. P.; Leopold, M. C.; Hicks, J. F.; Kulesza, P. J.; Malik, M. A.; Murray, R. W. *J. Am. Chem. Soc.* **2002**, *124*, 8958–8964.
(8) Rudoy, V. M.; Ershov, B. G.; Sukhov, N. L.; Dement'eva, O. V.; Zaitseva, A. V.; Seliverstov, A. F.; Kartseva, M. E.; Ogarev, V. A. *Colloid J.* **2002**, *64*, 755–758.
(9) Anyaogu, K. C.; Fedorov, A. V.; Neckers, D. C. *Langmuir* **2008**, *24*, 4340–4346.
(10) Cioffi, N.; Torsi, L.; Ditaranto, N.; Tantillo, G.; Ghibelli, L.; Sabbatini, L.; Bleve-Zacheo, T.; D'Alessio, M.; Zambonin, P. G.; Traversa, E. *Chem. Mater.* **2005**, *17*, 5255–5262.
(11) Sambhy, V.; MacBride, M. M.; Peterson, B. R.; Sen, A. *J. Am. Chem. Soc.* **2006**, *128*, 9798–9808.
(12) Balan, L.; Burget, D. *Eur. Polym. J.* **2006**, *42*, 3180–3189.
(13) Selvan, T.; Spatz, J. P.; Klok, H.; Möller, M. *Adv. Mater.* **1998**, *10*, 132–134.
(14) (a) Gaddy, G. A.; Korchev, A. S.; McLain, J. L.; Slaten, B. L.; Steigerwalt, E. S.; Mills, G. *J. Phys. Chem. B* **2004**, *108*, 14850–14857. (b) Lu, Y.; Mei, Y.; Schrinner, M.; Ballauff, M.; Moller, M. W.; Breu, J. *J. Phys. Chem. C* **2007**, *111*, 7676–7681.
(15) Nub, S.; Bottchen, H.; Wurm, H.; Hallensleden, M. L. *Angew. Chem., Int. Ed.* **2001**, *40*, 4016–4018.
(16) Mandal, T. K.; Fleming, M. S.; Walt, D. R. *Nano Lett.* **2002**, *2*, 3–7.
(17) Corbierre, M. K.; Cameron, N. S.; Sutton, M.; Mochrie, S. G. J.; Lurio, L. B.; Ruhm, A.; Lennox, R. B. *J. Am. Chem. Soc.* **2001**, *123*, 10411–10412.
(18) Korchev, A. S.; Bozack, M. J.; Slaten, B. L.; Mills, G. *J. Am. Chem. Soc.* **2004**, *126*, 10–11.
(19) Sangermano, M.; Yagci, Y.; Rizza, G. *Macromolecules* **2007**, *40*, 8827–8829.
(20) (a) Rong, M. Z.; Zhand, M. Q.; Ruan, W. H. *Mater. Sci. Technol.* **2006**, *22*, 787–796. (b) Hooper, J. B.; Schweizer, K. S. *Macromolecules* **2006**, *39*, 5133–5142.
(21) Cai, X.; Anyaogu, K. C.; Neckers, D. C. *J. Am. Chem. Soc.* **2007**, *129*, 11324–11325.
(22) Baauerle, P.; Wuerthner, F.; Goetz, G.; Effenberger, F. *Synthesis* **1993**, *11*, 1099–1103.
(23) Sotgiu, G.; Zambianchi, M.; Barbarella, G.; Botta, C. *Tetrahedron* **2002**, *58*, 2245–2251.
(24) Brust, M.; Walker, M.; BethelL, D.; Schiffrin, D. T.; Whyman, R. *J. Chem. Soc., Chem. Commun.* **1994**, 801–802.
(25) Leff, D. V.; Ohara, P. C.; Heath, J. R.; Gelbart, W. M. *J. Phys. Chem.* **1995**, *99*, 7036–7041.
(26) Ermoshkin, A. A.; Neckers, D. C.; Fedorov, A. V. *Macromolecules* **2006**, *39*, 5669–5674.
(27) Grinevich, O.; Snavely, D. L. *Chem. Phys. Lett.* **1999**, *304*, 202–206.
(28) (a) Evans, C. H.; Scaiano, J. C. *J. Am. Chem. Soc.* **1990**, *112*, 2694–2701. (b) Caspar, J. V.; Ramamurthy, V.; Corbin, D. R. *J. Am. Chem. Soc.* **1991**, *113*, 600–610. (c) Wintgens, V.; Valat, P.; Garnier, F. *J. Phys. Chem.* **1994**, *98*, 228–232. (d) Grage, M. M. L.; Keszthelyi, T.; Offersgard, J. F.; Wilbrandt, R. *Chem. Phys. Lett.* **1998**, *282*, 171–175. (e) Yagci, Y.; Jockusch, S.; Turro, N. J. *Macromolecules* **2007**, *40*, 4481–4485.
(29) (a) Moeller, K. D. *Tetrahedron* **2000**, *56*, 9527–9554. (b) Brumfield, M. A.; Quillen, S. L.; Yoon, U. C.; Mariano, P. S. *J. Am. Chem. Soc.* **1984**, *106*, 6855–6856. (c) Seiders, J. R.; Wang, L.; Floreancig, P. E. *J. Am. Chem. Soc.* **2003**, *125*, 2406–2407.
(30) (a) Johnston, L. J.; Schepp, N. P. *J. Am. Chem. Soc.* **1993**, *115*, 6564–6571. (b) Baciocchi, E.; Bietti, M.; Lanzalunga, O. *Acc. Chem. Res.* **2000**, *33*, 243–251. (c) Lida, K.; Yoshida, K. *Macromolecules* **2006**, *39*, 6420–6424.
(31) Gu, T.; Whitesell, J. K.; Fox, M. A. *Chem. Mater.* **2003**, *15*, 1358–1366.
(32) Guyard, L.; Hapiot, P.; Jouini, M.; Lacroix, J.-C.; Lagrost, C.; Neta, P. *J. Phys. Chem. A* **1999**, *103*, 4009–4015.
(33) Shah, B. K.; Neckers, D. C. *J. Am. Chem. Soc.* **2004**, *126*, 1830–1835, and references therein.
(34) Sartomer Company, Inc., Exton, PA, http://sartomer.com.
(35) Link, S.; El-Sayed, M. A. *Int. Rev. Phys. Chem.* **2000**, *19*, 409–453.
(36) (a) Starr, F. W.; Schroder, T. B.; Glotzer, S. C. *Macromolecules* **2002**, *35*, 4481–4492. (b) Hooper, J. B.; Schweizer, K. S. *Macromolecules* **2006**, *39*, 5133–5142.
(37) (a) Tyagi, S.; Lee, J. Y.; Buxton, G. A.; Balazs, A. C. *Macromolecules* **2004**, *37*, 9160–9168. (b) Mackay, M. E.; Tuteja, A.; Duxbury, P. M.; Hawker, C. J.; Van Horn, B.; Guan, Z.; Chen, G.; Krishnan, R. S. *Science* **2006**, *311*, 1740–1743.

MA801391P